Cosmic Magnetic Fields:
From Planets, to Stars and Galaxies
Proceedings IAU Symposium No. 259, 2008
K.G. Strassmeier, A.G. Kosovichev & J. Beckman, eds.

doi:10.1017/S1743921309030749

Magnetic fields in White Dwarfs and their direct progenitors

Stefan Jordan

Astronomisches Rechen-Institut, Zentrum für Astronomie, Mönchhofstr. 12-14,
D-69120 Heidelberg, Germany
email: jordan@ari.uni-heidelberg.de

Abstract. The paper provides an overview on the results of the analyses of spectro-polarimetric observations of white dwarfs, subdwarfs, and central stars of planetary nebulae. It will also discuss the question of the origin of the magnetic fields in white dwarfs.

Keywords. White Dwarfs – magnetic fields – subdwarfs – Planetary Nebulae

1. Introduction and history

Blackett (1947) predicted that very strong magnetic fields (≈ 1 MG) could exist in white dwarfs if the magnetic moment of a star is proportional to its angular momentum, which he assumed to be conserved during the stellar evolution and the collapse. This is, however, probably not the case since most isolated white dwarfs seem to be relatively slow rotators ($v \lesssim 40$ km/sec, see Karl *et al.* 2005 and references thererein), although a few exceptions from this rule exist (e.g. RE J 0317-853 with a rotational period of 725 sec, Barstow *et al.* 1995); if angular momentum were completely conserved during the evolution we would expect the white dwarf remnant to have $v_{rot} \approx 10,000$ km/sec.

Another possibility was proposed by Ginzburg (1964) and Woltjer (1964). They argued that if the magnetic flux, which is proportional to BR^2, is conserved during evolution and collapse, very strong magnetic fields can be reached in degenerate stars. A main sequence star with a radius $R \approx 10^{11}$ cm and a surface magnetic field of 1-10 kG can therefore become a white dwarf ($R \approx 10^9$ cm) with a magnetic field strength of 10^7-10^8 G.

The search for magnetic white dwarfs began in 1970 when Preston looked for quadratic Zeeman shifts in the spectra of DA white dwarfs. Due to the extremely strongly Stark broadened Balmer lines and the limited spectral resolution he was only able to place upper limits of about 0.5 MG for the magnetic fields in several white dwarfs. A rather sensitive method to detect magnetic fields in white dwarfs is the measurement of circular polarization. Kemp (1970) detected circular polarization of several percent in Grw +70°8247, an object that was known for its rather shallow and unidentified "Minkowski bands" (Minkowski 1938). Although his derived value for the magnetic field strength was wrong this proved the existence of a magnetic field in this white dwarf. Nevertheless, all attempts to identify the Minkowski bands with various atoms or molecules in magnetic fields of a few MG failed.

Even for the simplest atoms, hydrogen and helium, accurate calculations for the line components did not exist at that time for field strengths above 20-100 MG (Kemic 1974a,b); only for extremely intense fields (10^9-10^{10} G) data were available again Garstang (1977), but none of the predicted line positions were in agreement with the wavelengths of the Grw +70°8247 features. For this reason Angel (1979) proposed that the star must possess a field strength above 100 MG (but below the intense-field regime).

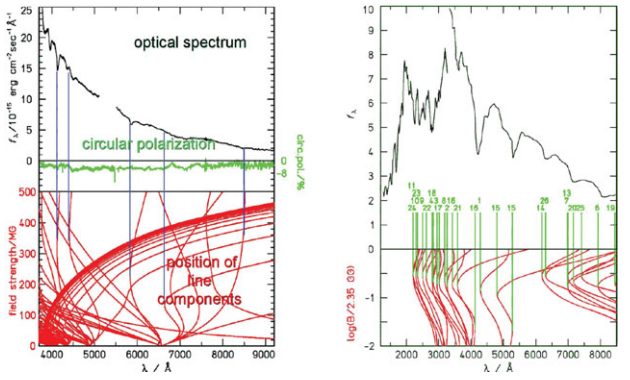

Figure 1. Spectrum and circular polarisation of the famous magnetic white dwarf Grw +70°8247 (left) can the identification of the spectral features with stationary line components; the dipole field strength is ≈ 320 MG (Jordan 1992). On the right hand side, the spectrum of GD 229 is compared to stationary line components of neutral helium (Jordan *et al.* 1998).

For hydrogen the intermediate-field gap has been closed more than twenty years ago with calculations of energy level shifts and transition probabilities for bound-bound transitions by groups in Tübingen and Baton Rouge (Forster *et al.* 1984; Rösner *et al.* 1984; Henry & O'Connell 1984).

2. Stationary line components

Since the magnetic field on the surface of a white dwarf normally is not homogeneous but e.g. better described by a magnetic dipole or more complicated field geometries, the variation of the field strengths from the pole to the equator (a factor of two for a pure dipole field) smears out most of the absorption lines; this explains why the spectral features on Grw +70°8247 are so shallow. However, a few of the line components become stationary, i.e. their wavelengths go through maxima or minima as functions of the magnetic field strength. These stationary components are visible in the spectra of magnetic white dwarfs despite a considerable variation of the field strengths.

It was a great confirmation for the correctness of the theoretical calculations that indeed the unidentified features in the optical and UV spectrum of Grw +70°8247 could be attributed to stationary components of hydrogen (see Fig. 1) in fields between about 150 and 500 MG (Greenstein 1984; Greenstein *et al.* 1985).

For helium reliable atomic data for arbitrary magnetic field strengths became available only in the late nineties (see Jordan *et al.* 1998, 2001) when the existence of helium could be proven (Jordan *et al.* 1998).

Table 1: List of all known MWDs, extending the one by Kawka *et al.* (2007), containing the name of the object, the effective temperature, the chemical composition, the magnetic field strength (usually the dipole field strength), the rotational period. References are provided only if not provided by Kawka *et al.* (2007). For uncertainties of the values please refer to the original papers.

Object	$T_{\rm eff}$/kK	Comp.	B/MG	$P_{\rm rot}$	References
SDSS J000555.91−100213.4	29000	He/C	?	···	
LHS 1038	6540	H	$\lesssim$0.2	$>$ 2 h	
LHS 1044	6010	H	16.7	···	
SDSS J001742.44+004137.4	15000	He	8.30	···	
SDSS J002129.00+150223.7	7000	H	530.69	···	Külebi *et al.* (08)
SDSS J004248.19+001955.3	11000	H	2.00	···	Külebi *et al.* (08)
Feige 7	20000	H/He	35.00	12 m	

https://doi.org/10.1017/S1743921309030749 Published online by Cambridge University Press

Table 1: continued.

Object	$T_{\rm eff}$/kK	Comp.	B/MG	$P_{\rm rot}$	References
SDSS J014245.37+131546.4	15000	He	4.00	···	
SDSS J015748.15+003315.1	$\sim$ 6000	He (DZ)	3.70	···	
MWD 0159−032	26000	H	6.00	···	
SDSS J021116.34+003128.5	9000	H	341.31	···	Külebi *et al.* (08)
SDSS J021148.22+211548.2	12000	H	168.20	···	Külebi *et al.* (08)
SDSS J023609.40−080823.9	10000	H (DQA)	5.00	···	
HE 0236−2656	6500	He	?	···	
HE 0241−155	12000	H	200	···	Reimers *et al.* (04)
KPD 0253+5052	15000	H	13.5	···	
LHS 5064	6680	H	$\sim$ 0.1	···	
SDSS J030407.40−002541.7	15000	H	10.95	···	Külebi *et al.* (08)
MWD 0307−428	25000	H	10.00	···	
SDSS J031824.19+422651.0	10500	H	10.12	···	Külebi *et al.* (08)
REJ J0317−853	33000	H	$>$ 180	725 s	
KUV 03292+0035	26500	H	12.10	···	
HE 0330−0002	6500	He	?	···	
SDSS J033145.69+004517.0	15500	H	13.13	···	Külebi *et al.* (08)
SDSS J034308.18−064127.3	13000	H	19.78	···	Külebi *et al.* (08)
SDSS J034511.11+003444.3	8000	H	1.96	···	Külebi *et al.* (08)
40 Eri B	16490	H	0.0023	···	
BPM 3523	23450	H	0.00428	···	
LHS 1734	5300	H	7.3	···	
G 99−37	6070	C_2/CH	7.5	4.1 h	Berd. *et al.* (07)
G 99−47	5790	H	20	0.97 h	
EUVE J0616−649	50000	H	14.80	···	
GD 77	14870	H	1.2	···	
G 234−4	4500	H	0.0396	···	
SDSS J074850.48+301944.8	22000	H	6.75	···	Külebi *et al.* (08)
SDSS J075234.96+172525.0	9000	H	10.30	···	Külebi *et al.* (08)
SDSS J075819.57+354443.7	22000	H	26.40	···	Külebi *et al.* (08)
G 111−49	8500	H	220	···	
SDSS J080440.35+182731.0	11000	H	48.47	···	Külebi *et al.* (08)
SDSS J080502.29+215320.5	28000	H	6.11	···	Külebi *et al.* (08)
SDSS J080743.33+393829.2	13000	H	65.75	···	Külebi *et al.* (08)
SDSS J080938.10+373053.8	14000	H	39.74	···	Külebi *et al.* (08)
SDSS J081648.71+041223.5	11500	H	7.35	···	Külebi *et al.* (08)
GD 90	14000	H	9.00	···	
EUVE J0823−254	43200	H	2.8 − 3.5	···	
SDSS J082835.82+293448.7	19500	H	33.40	···	Külebi *et al.* (08)
EG 61	17100	H	$\sim$ 3	···	
SDSS J084008.50+271242.7	12250	H	3.38	···	Külebi *et al.* (08)
SDSS J084155.74+022350.6	7000	H	5.00	···	Külebi *et al.* (08)
SDSS J083945.56+200015.7	15000	H	3.38	···	
SDSS J084716.21+484220.4	19000	H	$\sim$ 3	···	

https://doi.org/10.1017/S1743921309030749 Published online by Cambridge University Press

Table 1: continued.

Object	$T_{\rm eff}$/kK	Comp.	B/MG	$P_{\rm rot}$	References
SDSS J085106.12+120157.8	11000	H	2.03	···	Külebi *et al.* (08)
LB 8915	24000	H/He	0.75 − 1.0	···	
SDSS J085523.87+164059.0	15500	H	12.23	···	Külebi *et al.* (08)
SDSS J085830.85+412635.1	7000	H	3.38	···	Külebi *et al.* (08)
SDSS J090632.66+080716.0	17000	H	10.00	···	
SDSS J090746.84+353821.5	16500	H	22.40	···	Külebi *et al.* (08)
SDSS J091124.68+420255.9	10250	H	35.20	···	Külebi *et al.* (08)
SDSS J091437.40+054453.3	17000	H	9.16	···	Külebi *et al.* (08)
G 195−19	7160	He	∼ 100	1.3 d	
SDSS J091833.32+205536.9	14000	H	2.04	···	Külebi *et al.* (08)
SDSS J092527.47+011328.7	10000	H	2.04	···	Külebi *et al.* (08)
SDSS J093313.14+005135.4	···	He (C_2H)?	?	···	
SDSS J093356.40+102215.7	8500	H	2.11	···	Külebi *et al.* (08)
SDSS J093447.90+503312.2	8900	H	9.50	···	Külebi *et al.* (08)
SDSS J094458.92+453901.2	15500	H	15.91	···	
LB 11146	16000	H	670.00	···	
SDSS J095442.91+091354.4	···	DQ	?	···	
SDSS J100005.67+015859.2	9000	H	19.74	···	Külebi *et al.* (08)
SDSS J100356.32+053825.6	23000	H	10.13	···	Külebi *et al.* (08)
SDSS J100657.51+303338.1	10000	H	1.00	···	Külebi *et al.* (08)
SDSS J100715.55+123709.5	18000	H	5.41	···	Külebi *et al.* (08)
LHS 2229	4600	He (C_2H)	∼ 100	···	
SDSS J101529.62+090703.8	7200	H	4.09	···	Külebi *et al.* (08)
SDSS J101618.37+040920.6	10000	H	7.94	···	Külebi *et al.* (08)
PG 1015+014	14000	H	70.00	99 m	Euchner *et al.* (06)
GD 116	16000	H	65	···	
SDSS J102239.06+194904.3	9000	H	2.94	···	Külebi *et al.* (08)
LHS 2273	7160	H	18.00	···	
PG 1031+234	∼ 15000	H	≲1000	3.4 h	
SDSS J103655.38+652252.0	···	DQ	0.17	···	
LP 790−29	7800	He	50.00	26 y?	
HE 1043−0502	∼ 15000	He	∼ 820	···	
HE 1045−0908	10000	H	16.00	2.7 h	
SDSS J105404.38+593333.3	9500	H	17.63	···	Külebi *et al.* (08)
SDSS J105628.49+652313.5	16500	H	29.27	···	Külebi *et al.* (08)
LTT 4099	15280	H	0.0039	···	
SDSS J111010.50+600141.4	30000	H	6.37	···	Külebi *et al.* (08)
SDSS J111341.33+014641.7	···	He ?	?	···	
SDSS J111812.67+095241.4	10500	H	3.38	···	Külebi *et al.* (08)
SDSS J112257.10+322327.8	12500	H	11.38	···	Külebi *et al.* (08)
SDSS J112852.88−010540.8	11000	H	2.00	···	Külebi *et al.* (08)
SDSS J112924.74+493931.9	10000	H	5.31	···	
SDSS J113357.66+515204.8	22000	H	8.64	···	Külebi *et al.* (08)
SDSS J113756.50+574022.4	7800	H	5.00	···	Külebi *et al.* (08)

https://doi.org/10.1017/S1743921309030749 Published online by Cambridge University Press

Table 1: continued.

Object	$T_{\rm eff}$/kK	Comp.	B/MG	$P_{\rm rot}$	References
LBQS 1136−0132	10500	H	22.71	···	
SDSS J114006.37+611008.2	13500	H	50.19	···	Külebi *et al.* (08)
SDSS J114829.00+482731.2	27500	H	32.47	···	Külebi *et al.* (08)
SDSS J115418.14+011711.4	1125	H	33.47	···	Külebi *et al.* (08)
SDSS J115917.39+613914.3	23000	H	20.10	···	Külebi *et al.* (08)
SDSS J120150.10+614257.0	10500	H	11.35	···	Külebi *et al.* (08)
SDSS J120609.80+081323.7	13000	H	760.63	···	Külebi *et al.* (08)
SDSS J120728.96+440731.6	16750	H	2.03	···	Külebi *et al.* (08)
SDSS J121209.31+013627.7	10000	H	10.12	···	Külebi *et al.* (08)
HE 1211−1707	∼ 12000	He	50.00	∼ 2 h	
LHS 2534	6000	He (DZ)	1.92	···	
SDSS J121635.37−002656.2	20000	H	59.70	···	Külebi *et al.* (08)
SDSS J122209.44+001534.0	20000	H	14.70	···	Külebi *et al.* (08)
PG 1220+234	26540	H	3.00	···	
SDSS J122249.14+481133.1	9000	H	8.05	···	Külebi *et al.* (08)
SDSS J122401.48+415551.9	9500	H	22.36	···	Külebi *et al.* (08)
SDSS J123414.11+124829.6	8200	H	4.32	···	Külebi *et al.* (08)
SDSS J124806.38+410427.2	7000	H	7.03	···	Külebi *et al.* (08)
SDSS J124851.31−022924.7	13500	H	7.36	···	Külebi *et al.* (08)
SDSS J125044.42+154957.4	10000	H	20.71	···	Külebi *et al.* (08)
SDSS J125416.01+561204.7	13250	H	38.86	···	Külebi *et al.* (08)
HS 1254+3440	15000	H	9.5	···	
SDSS J125434.65+371000.1	10000	H	4.10	···	Külebi *et al.* (08)
SDSS J125715.54+341439.3	8500	H	11.45	···	Külebi *et al.* (08)
G 256−7	∼ 56000	H	4.9	···	
PG 1312+098	∼ 20000	H	10.00	5.4 h	
SDSS J132002.48+131901.6	14750	H	2.02	···	Külebi *et al.* (08)
SDSS J132858.20+590851.0	25000	H (DQA)	18.00	···	
G165-7	6440	He (DZ)	0.65	···	
G 62−46	6040	H	7.36	···	
SDSS J133359.86+001654.8	···	He (C_2H)?	?	···	
SDSS J133340.34+640627.4	13500	H	10.71	···	Külebi *et al.* (08)
SDSS J134043.10+654349.2	15000	H	4.32	···	Külebi *et al.* (08)
SDSS J134820.79+381017.2	35000	H	13.65	···	Külebi *et al.* (08)
SBS 1349+5434	11000	H	760	···	
LP 907−037	9520	H	$\lesssim$0.3	···	
SDSS J140716.66+495613.7	20000	H	12.49	···	Külebi *et al.* (08)
SDSS J141906.19+254356.5	9000	H	2.03	···	Külebi *et al.* (08)
SDSS J142625.71+575218.3	19830	He/C_2 (DQ)	∼ 1.2	···	Dufour *et al.* (08)
SDSS J142703.40+372110.5	19000	H	27.04	···	Külebi *et al.* (08)
SDSS J143019.05+281100.8	9000	H	9.34	···	Külebi *et al.* (08)

https://doi.org/10.1017/S1743921309030749 Published online by Cambridge University Press

Table 1: continued.

Object	$T_{\rm eff}$/kK	Comp.	B/MG	$P_{\rm rot}$	References
SDSS J143218.26+430126.7	24000	H	2.04	···	Külebi *et al.* (08)
SDSS J143235.46+454852.5	16750	H	12.29	···	Külebi *et al.* (08)
EUVE J1439+750	$>$ 20000	H	14 − 16	···	
SDSS J144614.00+590216.7	12500	H	4.42	···	Külebi *et al.* (08)
SDSS J145415.01+432149.5	11500	H	2.35	···	Külebi *et al.* (08)
GD 175	6990	H	2.30	···	
SDSS J150813.20+394504.9	17000	H	13.23	···	Külebi *et al.* (08)
SDSS J151130.20+422023.0	9750	H	22.40	···	Külebi *et al.* (08)
SDSS J151745.19+610543.6	9500	H	13.98	···	Külebi *et al.* (08)
GD 185	18620	H	0.035	···	
PG 1533−057	20000	H	31	···	
SDSS J153532.25+421305.6	18500	H	5.27	···	Külebi *et al.* (08)
SDSS J153829.29+530604.6	13500	H	13.99	···	Külebi *et al.* (08)
SDSS J154213.48+034800.4	8500	H	8.35	···	Külebi *et al.* (08)
SDSS J160437.36+490809.2	9000	H	59.51	···	Külebi *et al.* (08)
GD 356	7510	He	13.00	0.1 d	
SDSS J164357.02+240201.3	16500	H	2.00	···	Külebi *et al.* (08)
SDSS J164703.24+370910.3	16250	H	2.10	···	Külebi *et al.* (08)
SDSS J165029.91+341125.5	9750	H	3.38	···	Külebi *et al.* (08)
SDSS J165203.68+352815.8	11500	H	7.37	···	Külebi *et al.* (08)
PG 1658+440	30510	H	2.3	···	
SDSS J170400.01+321328.7	23000	H	50.11	···	Külebi *et al.* (08)
NLTT 44447	6260	H	1.30	···	
SDSS J171556.29+600643.9	13500	H	2.03	···	Külebi *et al.* (08)
SDSS J172045.37+561214.9	22500	H	19.79	···	Külebi *et al.* (08)
SDSS J172329.14+540755.8	16500	H	32.85	···	Külebi *et al.* (08)
SDSS J172932.48+563204.1	10500	H	27.26	···	Külebi *et al.* (08)
BPM 25114	$\sim$ 20000	H	36.00	2.8 d	
G 240−72	5590	He	$\gtrsim$100	$\gtrsim$20 y	
G 183−35	6500	H	$\sim$ 14	$\sim$ 50 m?	
G 141−2	6340	H	$\sim$ 3	···	
G 227−35	6280	H	175	···	
Grw +70°8247	16000	H	320	···	
G 92−40	7920	H	$\gtrsim$0.1	1.4 d	
GD 229	18000	He	700	···	Jordan *et al.* (98)
LTT 7987	15360	H	0.001	···	Jordan *et al.* (07)
SDSS J202501.10+131025.6	17000	H	10.10	···	Külebi *et al.* (08)
SDSS J204626.15−071037.0	8000	H	2.03	···	Külebi *et al.* (08)
SDSS J205233.52−001610.7	19000	H	13.42	···	Külebi *et al.* (08)
L 24−52	10200	H	0.043 ?	···	
SDSS J214900.87+004842.8	11000	H	10.09	···	Külebi *et al.* (08)
SDSS J214930.74−072812.0	22000	H	44.71	···	Külebi *et al.* (08)
SDSS J215135.00+003140.5	9000	H	$\sim$ 300	···	Külebi *et al.* (08)
SDSS J215148.31+125525.5	14000	H	20.76	···	Külebi *et al.* (08)
SDSS J220435.05+001242.9	22000	H	1.02	···	Külebi *et al.* (08)
SDSS J221828.59−000012.2	15500	H	225.00	···	

https://doi.org/10.1017/S1743921309030749 Published online by Cambridge University Press

Table 1: continued.

Object	$T_{\rm eff}$/kK	Comp.	B/MG	$P_{\rm rot}$	References
SDSS J224741.46+145638.8	18000	H	42.11	···	Külebi *et al.* (08)
SDSS J225726.05+075541.7	40000	H	16.17	···	Külebi *et al.* (08)
KUV 813−14	11000	H	45	18 d	
SDSS J231951.73+010909.3	8300	H	9.35	···	Külebi *et al.* (08)
SDSS J232248.22+003900.9	39000	H	21.40	···	Külebi *et al.* (08)
SDSS J232337.55−004628.2	15000	He	4.80	···	
PG 2329+267	9400	H	2.31	···	
SDSS J234623.69−102357.0	8500	H	9.17	···	Külebi *et al.* (08)
SDSS J234605.44+385337.7	26000	H	1000.00	···	
LTT 9857	8570	H	0.0031	···	

3. Modelling spectra and polarisation of magnetic white dwarfs

These identifications with stationary line components allowed an estimation of the approximate range of field strengths covering the stellar surface. However, the detailed field structure could not be inferred. This was only possible by simulating the radiative transfer through a magnetized stellar atmospheres, as e.g. described by Jordan (1992). In order to calculate theoretical flux and polarisation spectra for a given geometry of the magnetic field, theoretical Stokes parameters have to be evaluated on a few hundred surface elements taking into account the local magnetic field strength and the orientation of the magnetic field with respect to the observer and the normal of the stellar surface. Afterward, the results from the respective surface elements must be summed up.

Such a forward calculation for a given magnetic field geometry is relatively simple. The goal, however, is to determine the magnetic field geometry from the observed spectra and polarisation data. Since it turned out that most magnetic white dwarfs could not be described by simple dipole fields (see eg. Achilleos & Wickramasinghe 1989), the number of free parameters to describe the field geometry can be very large. Therefore, finding a magnetic field geometry that adequately reproduces the observed spectro-polarimetric data is extremely tedious and practically impossible when time resolved observations of rotating magnetic white dwarfs are used that have to reproduce the observation for all different rotational phases.

For the first time Burleigh *et al.* (1999) used an automatic least-squares fit procedure to determine the magnetic field geometry of RE J 0317-853 from phase resolved HST data (see Fig. 3) They used a downhill simplex method in multidimensions to account for the rotational geometry and an assumed offset-dipole configuration of the magnetic field. However, the approach has the disadvantage of easily running into local minima rather than the global χ^2 minimum of the high-dimensional parameter space. It also turned out that the optical spectro-polarimetric data of RE J 0317-853 are not fully consistent with the geometry derived from the UV data so that more sophisticated fit procedures need to be used.

A rather successful approach is the application of genetic (Jordan) and evolutionary (Euchner) algorithms to find a magnetic field geometry that is consistent with the spectro-polarimetric data of for all rotational phases (Euchner *et al.* 2002; Gänsicke *et al.* 2002; Euchner *et al.* 2005, 2006; Beuermann *et al.* 2007).

https://doi.org/10.1017/S1743921309030749 Published online by Cambridge University Press

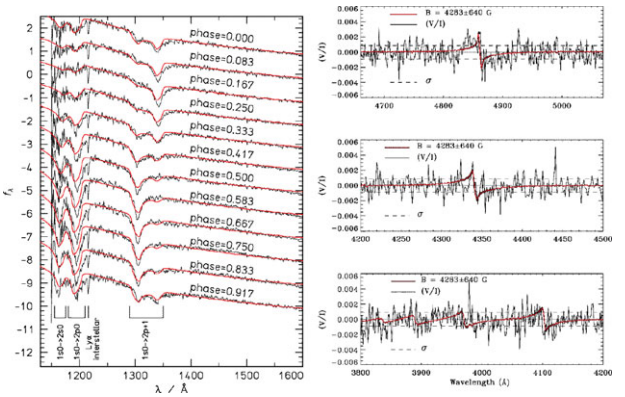

Figure 2. Left side: Observed and theoretical spectra UV spectra for 12 different phase across the 725 s rotation period of RE J 0317-853 for a magnetic dipole with a polar field strength of 363 MG, shifted by 0.19 stellar radii along the dipole axis (Burleigh *et al.* 1999). Right: Measurement of a 4.3 kG magnetic field in the white dwarf WD 446−789.

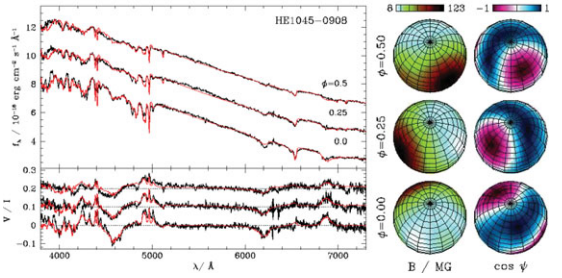

Figure 3. Zeeman tomography analysis of the magnetic field configuration of HE 1045−0908 using a dipole/quadrupole combination. B is the magnetic field strength and ψ is the angle between the local magnetic field vector and the observer.

4. Chemical species other than hydrogen

All really detailed analyses of magnetic white dwarfs were limited to those with hydrogen-rich atmospheres. The reason is that atomic data for helium have not consistently been included into our radiative transfer models yet. First tentative analyses using the new helium data were, however, performed by Wickramasinghe *et al.* (2002).

In some cool ($T_{\rm eff} < 9000$ K) helium rich magnetic white dwarfs, carbon molecules (C_2, CH) are responsible for the absorption. Bues & Pragal (1989) have interpreted such spectra with very simple approximations of the molecular physics of the Swan bands of C_2 in magnetic fields between 10 and 150 MG. Berdyugina *et al.* (2007) has used a Paschen-Back approximation for the C_2 absorption but has not yet analyse such objects with state-of-the-art radiation transfer models.

One of the most exciting recent discoveries is the detection of non-radial pulsations in a magnetic white dwarf with a hot carbon-rich atmosphere (Dufour *et al.* 2008).

5. Magnetic white dwarfs with high magnetic fields

About 10% of all isolated white dwarfs posses surface magnetic fields of more that 10^6 G (Liebert J. *et al.* 2005). Generally, magnetic white dwarfs with MG fields tend to be more massive than non-magnetic ones (Liebert J. 1988), but the number of objects with reliable mass determinations is rather small.

The Sloan Digital Sky Survey (SDSS) has almost tripled the number of known white dwarfs with MG fields (Schmidt *et al.* 2003; Vanlandingham *et al.* 2005). Külebi *et al.* (2008) have analysed all hydrogen-rich magnetic white dwarfs and found that almost all objects show indications field geometries which are more complicated than centered magnetic dipoles (see also Külebi *et al.* in these proceedings). The list of all currently know magnetic white dwarfs is provided in Table. 1.

https://doi.org/10.1017/S1743921309030749 Published online by Cambridge University Press

6. Kilogauss magnetic fields in white dwarfs and their progenitors

Until recently, magnetic fields below 30 kG could not be detected, with the exception of the very bright white dwarf 40 Eri B ($V = 8.5$), in which Fabrika *et al.* (2003) found a magnetic field of 4 kG. However, by using the ESO VLT, we could push the detection limit down to about 1 kG in two investigations of 22 DA white dwarfs with $11 < V < 14$ (Aznar Cuadrado *et al.* 2004; Jordan *et al.* 2007) by means of polarimetry. The degree of polarization in the vicinity of the spectral lines caused by 1 kG is only about 0.1% (see Fig. 3 as an example).

Magnetic fields of kilogauss strength have also been detected in the direct progeny of white dwarfs – central stars of planetary nebulae Jordan *et al.* (2005), probably the channel leading to about 99% of all white dwarfs, and hot subdwarfs O'Toole *et al.* (2005), accounting for about 1%. The magnetic fields found were between 1 and 3 kG. If the magnetic flux is fully conserved during the transition phase to white dwarfs – these objects will become magnetic white dwarfs with fields up to 2 MG.

However, great care is necessary, since these detections in central stars and subdwarfs are at the very limit of what is observationally possible. Together with new observations of central stars of planetary nebular we are also checking the data analysis again in order to be convinced that the detections are real.

7. Origin of magnetic white dwarfs

The strong magnetic fields can be fossil if the magnetic flux is conserved during stellar evolution. The very high electric conductivity of degenerate electron gas in the interior of white dwarfs leads to very long decay times ($\gtrsim 10^{10}$ yr). For a long time it was assumed that the higher modes decay more rapidly than the fundamental (Chanmugam *et al.* 1972; Fontaine *et al.* 1973). However, Muslimov *et al.* (1995) have shown that a weak quadrupole (or octupole, etc.) component on the surface magnetic field of a white dwarf may survive the dipole component and specific initial conditions: Particularly the evolution of the quadrupole mode is very sensitive (via Hall effect) to the presence of internal toroidal field. Under certain conditions, the higher-order components of the magnetic field my survive as long as the dipole component.

This shows that, in principle, higher-order multipoles may give us some information about internal magnetization of white dwarfs and the initial conditions from the pre-white dwarf evolution. Therefore, further investigations of the complex magnetic fields of white dwarfs remain important.

The magnetic fluxes of the main-sequence stars with the highest magnetic fields are very similar to the highest magnetic fields found in magnetic white dwarfs (10^9 G). However, it is not easy to identify the main-sequence progenitors if we assume the fossil-field hypothesis, because magnetic fields below a few hundred Gauss are currently not detectable; moreover, magnetic fields in later type do not contain large-scale magnetic fields so that they also escape detection. The situation is also complicated by observational biases in the selection of the magnetic white dwarfs themselves. By applying initial-final mass relations and studying the number statistics Wickramasinghe & Ferrario (2005) concluded that magnetic white dwarfs cannot come from A_p and B_p stars alone.

Acknowledgements

I thank Baybars Külebi for his help preparing Table 1. The work on magnetic white dwarfs was supported by DLR project 50 OR 0802.

References

Achilleos, N. & Wickramasinghe, D. T. 1989, *ApJ* 346, 444

Angel J. R. P. 1979, in White Dwarfs and Variable Deg. Stars, Univ. of Rochester Press, p.313

Aznar Cuadrado, R., Jordan, S., Napiwotzki, R., Schmid, H. M., Solanki, S. K., & Mathys, G. 2004, *A&A* 423, 1081

Barstow, M. A., Jordan, S., O'Donoghue, D., Burleigh, M. R., Napiwotzki, R., & Harrop-Allin, M. K. 1995, *MNRAS* 277, 971

Berdyugina, S. V., Berdyugin, A. V., & Piirola, V. 2007, Phys. Rev. Lett. 99, 1101

Berdyugin, A. V. & Piirola, V. 1999, *A&A* 352, 619

Beuermann K., Euchner F., Reinsch K., Jordan S., & Gänsicke B. T. 2007, *A&A* 463, 647

Blackett P. M. S. 1947, *Nature* 159, 658

Bues, I. & Pragal, M. 1989, in White Dwarfs, Lecture Notes in Physics 328, ed. G. Wegner, p. 329

Burleigh, M. R., Jordan, S., & Schweizer, W. 1999, *ApJ* 510, L37

Chanmugam G. & Gabriel M. 1972, *A&A* 16, 149

Dufour, P., Fontain, G., Liebert, J., Williams, K., & Lai, D. K. 2008, *ApJ* 683, 167

Euchner F., Jordan S., Beuermann K., Gänsicke B., & Hessman F. V. 2002, *A&A* 390, 633

Euchner, F., Reinsch, K., Jordan, S., Beuermann, K., & Gänsicke, B. T. 2005, *A&A* 442, 651

Euchner, F., Jordan, S., Beuermann, K., Reinsch, K., & Gänsicke, B. T. 2006 *A&A* 451, 671

Fabrika S. N., Valyavin G. G., & Burlakova T. E. 2003, *Astronomy Letters* 29, 737

Fontaine G., Thomas J. H., & Van Horn H. M. 1973, *ApJ* 184, 911

Forster H., Strupat W., Rösner W., Wunner G., Ruder H., & Herold H. 1984, *J.Phys.* V 17, 1301

Garstang R. H. 1977, *Rep.Prog.Phys.* 40, 105

Gänsicke, B. T., Euchner, F., & Jordan, S. 2002, *A&A* 394, 957

Ginzburg V. L. 1964, *Sov. Phys. Dokl.* 9, 329

Greenstein J. L. 1984, *ApJ* 281, L47

Greenstein J. L., Henry R. J. W., & O'Connell R. F. 1985, *ApJ* 289, L25

Henry R. J. W. & O'Connell R. F. 1984, *ApJ* 282, L97

Jordan, S. 1992, *A&A*, 265, 570

Jordan, S., Schmelcher, P., & Becken W. 1998, *A&A*, 336, 33

Jordan, S., Schmelcher, P., Becken W., & Schweizer, W. 2001, *A&A* 376, 614

Jordan, S., Werner, K., & O'Toole, S. J. 2005, *A&A* 432, 273

Jordan, S., Aznar Cuadrado, R., Napiwotzki, R., Schmid, H. M., & Solanki, S. K. 2007, *A&A* 462, 1101

Karl, C. A., Napiwotzki, R., Heber, U., Dreizler, S., Koester, D., & Reid, I. N. 2005, *A&A* 434, 637

Kawka, A, Vennes, S, Schmidt G. D., Wickramasinghe D. T., & Koch R. 2007, *ApJ* 654, 499

Kemp J. C. 1970, *ApJ* 162, 169

Kemic S. B. 1974a, *ApJ* 193, 213

Kemic S. B. 1974b, JILA Rep. 133

Külebi, B., Jordan, S., Euchner F., Hirsch, H., & Löffler, W. 2008, Proceedings of the 16th European Workshop on White Dwarfs, Barcelona, in press

Liebert J. 1988, *PASP* 100, 1302

Liebert J. *et al.* 2005, *AJ* 129, 2376

Muslimov A. G., Van Horn H. M., & Wood M. A. 1995, *ApJ* 442, 758

O'Toole, S. J., Jordan, S., Friedrich, S., & Heber, U. 2005, *A&A* 437, 227

Preston G. W. 1970, *ApJ* 160, L143

Reimers, D., Jordan, S., & Christlieb, N. 2004, *A&A* 414, 1105

Rösner W., Wunner G., Herold H., & Ruder H. 1984, *J.Phys.* V 17, 29

Schmidt, G. D. *et al.* 2003, *ApJ* 595, 1101

Vanlandingham, K. M. *et al.* 2005, *AJ* 130, 734

Wickramasinghe, D. T., Schmidt, G. D., Ferrario, L., & Vennes, S. 2002, *MNRAS* 332, 29

Wickramasinghe, D. T. & Ferrario, L. 2005, *MNRAS* 356, 1576

Woltjer L. 1964, *ApJ* 140, 1309